

# Detection of Altered Collagen Fiber Alignment in the Cervical Facet Capsule After Whiplash-Like Joint Retraction

KYLE P. QUINN<sup>1</sup> and BETH A. WINKELSTEIN<sup>1,2</sup>

<sup>1</sup>Department of Bioengineering, University of Pennsylvania, 240 Skirkanich Hall, 210 S. 33rd St, Philadelphia, PA 19104-6321, USA; and <sup>2</sup>Department of Neurosurgery, University of Pennsylvania, Philadelphia, PA 19104, USA

(Received 4 February 2011; accepted 19 April 2011; published online 3 May 2011)

Associate Editor Stefan M. Duma oversaw the review of this article.

**Abstract**—The cervical facet joint has been identified as the source of pain in patients with whiplash-associated disorders, but most clinical studies report no radiographic evidence of tissue injury in these disorders. The goal of this study was to utilize quantitative polarized light imaging to assess the potential for altered collagen fiber alignment in human cadaveric cervical facet capsule specimens ( $n = 8$ ) during and after a joint retraction simulating whiplash exposure. Although no evidence of ligament damage was detected during whiplash-like retraction, mechanical and microstructural changes were identified after loading. Retraction produced significant decreases in ligament stiffness ( $p = 0.0186$ ) and increases in laxity ( $p = 0.0065$ ). In addition, image analysis indicated that  $21.1 \pm 17.1\%$  of the capsule sustained principal strains that were unrecovered immediately after retraction. Altered collagen fiber alignment was detected in  $32.7 \pm 22.9\%$  of the capsule after retraction. The capsule regions with unrecovered strain and altered fiber alignment after retraction were significantly co-localized with each other ( $p < 0.0001$ ), suggesting the altered mechanical function may relate to a change in the tissue's fiber organization. The identification of altered fiber alignment in this ligament following retraction without any tears implicates the whiplash kinematic as a potential cause of microstructural damage that is not detectable using standard clinical imaging techniques.

**Keywords**—Polarized light, Vector correlation, Ligament, Strain, Laxity, Fiber orientation, Facet joint.

## INTRODUCTION

The annual incidence of neck pain in the general population is estimated at nearly 20%, with chronic and debilitating symptoms for most individuals.<sup>3</sup>

Whiplash is a common cause of chronic neck pain, and the cervical facet joint has been identified as the site of pain in the majority of these cases.<sup>1</sup> Although anesthetic facet joint blocks, application of cytokine antagonists, and corticosteroid injections can provide temporary pain relief for some individuals,<sup>1,9,26</sup> up to 62% of people affected by whiplash injuries report pain lasting 2 years or more after injury.<sup>6</sup> Developing a fundamental understanding of facet joint injuries, and how to treat them following whiplash, has been impeded by the lack of radiographic or magnetic resonance imaging (MRI) evidence of any injury to the structures of the neck in most whiplash patients.<sup>2,19,21</sup> The lack of any definitive evidence of facet capsular ligament damage following whiplash, despite the high incidence of facet-mediated pain, suggests radiographic and MRI techniques may lack the resolution or contrast to identify these subtle injuries. Yet, no study has assessed the potential for changes in tissue microstructural organization of the facet capsule following whiplash-like loading.

Atypical cervical spine and facet joint motions have been identified during whiplash simulations.<sup>2,4,13,36</sup> Within 120 ms of bumper contact during a low-speed rear-end impact, the torso moves upward and forward, and the head extends backward,<sup>2,13</sup> causing the lower cervical spine to undergo a combination of compression, posterior shear, and extension.<sup>4,13</sup> This combination of forces and moments primarily induces a retraction of each vertebra in the posterior direction relative to its adjacent inferior vertebra in the lower cervical spine prior to head-headrest contact.<sup>4,28,29</sup> By tracking bony motions, studies have estimated that facet capsular ligament strains do, for some scenarios, exceed those strains measured during the cervical spine's normal range of motion.<sup>20,36</sup> These strain measurements suggest that the facet capsular ligament

Address correspondence to Beth A. Winkelstein, Department of Bioengineering, University of Pennsylvania, 240 Skirkanich Hall, 210 S. 33rd St, Philadelphia, PA 19104-6321, USA. Electronic mail: winkelst@seas.upenn.edu

may be at risk for excessive motion during vertebral retraction, but strain does not provide direct evidence of tissue damage that would indicate *if* and *under what conditions* facet capsule injury occurs during whiplash-like vertebral motions.

Isolated cervical spine studies have established the potential for subfailure injuries to the facet capsule following both mechanical failure tests and exposure to whiplash-like inertial spine loading.<sup>12,28,34,35</sup> Partial failures of the facet capsular ligament, defined by a transient decrease in load, do occur in some specimens prior to their gross rupture under tension or retraction. Partial failures do occur at capsule strain magnitudes that may be sustained during whiplash,<sup>28,34</sup> but this decrease in load does not consistently coincide with visible evidence of capsule damage.<sup>23</sup> Laxity in cervical facet capsular ligaments also has been identified after whiplash simulations.<sup>12</sup> Cryomicrotomy sections of a cervical spine following whiplash-like inertial loading also revealed facet joint diastasis.<sup>35</sup> Collectively, the increased gap between the articulating facets in the cryomicrotomy study and the detection of laxity following whiplash loading both suggest that the facet capsular ligament may sustain partial failures and/or unrecovered deformation during whiplash. *In vivo* models of facet joint injury indicate that altered collagen fiber organization and facet capsular ligament laxity may be produced following joint loading that produces persistent pain.<sup>16,18,22</sup> Furthermore, these *in vivo* studies demonstrate that neither partial failure nor capsule rupture is required to initiate facet-mediated pain,<sup>22</sup> suggesting painful facet joint injuries cannot be identified through traditional load-based or medical imaging techniques. Therefore, mechanistic studies are needed to understand the microstructural origins of facet capsular ligament damage and determine the potential for altered microstructural organization and laxity in the human facet capsule following whiplash-like facet retraction.

Polarized light has been utilized in many optical imaging studies to characterize the microstructural organization of the collagen fibers in soft tissue.<sup>14,31,33</sup> Atypical fiber realignment patterns of cadaveric and engineered tissue have been identified during the onset of tensile failure using a quantitative polarized light imaging (QPLI) technique that employs a rotating polarizer and circular analyzer.<sup>23,31</sup> More recently, a pixel-wise correlation calculation between fiber alignment vectors in sequential QPLI-derived alignment maps has been used to identify anomalous fiber realignment *during* loading of the facet capsular ligament.<sup>23</sup> The detection of anomalous fiber realignment prior to visible rupture or mechanical failure in that study was highly specific to a loss in tissue stiffness during loading, suggesting that the optical detection of

anomalous realignment may be a suitable surrogate marker for subfailure capsule injury.<sup>23</sup> Interestingly, the location of maximum principal strain measured during loading did not correspond to the location of damage predicted by anomalous fiber realignment, which suggests that the high spatial variability in fiber orientation of the capsule may produce substantial heterogeneity in its material properties.<sup>23</sup> Because anomalous fiber realignment was detected during tensile failure tests, it remains unknown whether permanent and detectable changes in collagen organization are produced when anomalous realignment is detected. Therefore, studies to evaluate whether the fiber alignment of the facet capsule is altered after a whiplash-like loading event are necessary to guide alternative approaches to diagnosing whiplash-induced facet joint damage in the clinic.

The goal of this study was to determine the potential for microstructural damage to the human facet capsular ligament during a whiplash simulation. To achieve this goal, a QPLI system was used to evaluate the collagen fiber kinematics *during* a whiplash-like retraction of cadaveric C6/C7 facet joints and to determine whether any ligament damage is evident *after* that loading by quantifying changes in fiber alignment and mechanical function. It was hypothesized that facet joint retraction produces anomalous realignment that results in unrecovered strain and altered fiber alignment after loading. Since retraction was hypothesized to induce unrecovered strain after retraction, the location of specific tissue regions was assumed to have changed between the alignment maps acquired before and after retraction. Therefore, a previously developed vector correlation tracking algorithm<sup>24</sup> was used to quantify both unrecovered tissue deformation and altered fiber alignment after retraction. To place the strain and fiber alignment measurements in the context of previous subfailure ligament biomechanical studies, changes to the mechanical response, such as ligament stiffness and laxity, were also evaluated through a cyclic tensile loading protocol performed both before and after the facet retraction.

## METHODS

### *Specimen Preparation*

Right and left facet joints ( $n = 8$ ) were obtained from five C6/C7 cervical spine motion segments from fresh, unembalmed human cadavers ( $58 \pm 12$  years of age). Fine dissection removed all musculature and tendon insertions on the surface of the facet capsule. Prior to the joint's isolation from the motion segment, two 0.4-mm holes were carefully drilled into each of

the C6 and C7 articular processes of the facet joints, and fiduciary pins (0.5 mm diameter shaft; 3.175 mm diameter spherical head) were manually inserted to define the natural in situ configuration for the joint to be used at the start of mechanical testing (Fig. 1). A digital image (18.52 pixels/mm resolution) of each joint with pins was acquired before it was removed en bloc, and the coordinates of the pins were digitized. The joint was further dissected removing the articular bone and cartilage along the medial–lateral axis to allow light transmission through the lateral aspect of the facet capsular ligament (Fig. 1). Using the digitized coordinates of the pins, the isolated specimens were positioned to simulate the positioning of the facet joint in the seated occupant, with a C6/C7 disc orientation of 21° below the horizontal (Fig. 1).<sup>34</sup>

#### General Specimen Loading Protocol

In order to assess microstructural and mechanical changes during and after a whiplash exposure, each specimen underwent facet retraction and a series of non-destructive tensile loading cycles imposed both before and after the retraction (Fig. 1). Accordingly, the C6 vertebra underwent 2.5 mm of retraction under displacement control in the posterior direction to simulate the magnitude of that joint's motion during the whiplash kinematic.<sup>28,29</sup> To evaluate whether the capsular ligament's mechanical response during activities of daily living is altered following whiplash-like retraction, cyclic tensile loading in the axial direction was applied before and after retraction to simulate the primary mode of loading for the ligament during normal sagittal bending of the cervical spine.<sup>30,37</sup> A customized testing interface was designed for an Instron 5385 (Instron; Norwood, MA) to enable both tensile and retraction loading of each specimen. For

specimens in either the tension or retraction configuration, C6 was displaced by the Instron crosshead, and a 100-N load cell recorded the load (with an accuracy of 0.25% of the measured value).

Each specimen underwent 30 cycles of tensile loading between 0 and 1 mm at 0.4 mm/s (Fig. 1) in order to produce a repeatable mechanical response of the capsular ligament to displacement of the C6 bone and to provide measurements for comparison to outcomes from the same loading performed after retraction. Such cyclic loading parameters were selected because neither ligament damage nor anomalous fiber realignment is produced for distractions up to 1 mm,<sup>23</sup> and the load generated by that distraction is approximately 5% of the tensile failure load of this ligament.<sup>34</sup> After cyclic loading, specimens were rotated 90°, maintaining the joint orientation, and were retracted (Fig. 1). C6 was retracted 2.5 mm at 0.4 mm/s, while QPLI images were collected at 500 Hz and a resolution of 18.52 pixels/mm using a Phantom v9.1 camera (Vision Research; Wayne, NJ), as previously described.<sup>23</sup> Previous whiplash simulation studies using human cadaveric specimens have estimated the magnitude of retraction of the lower cervical facet joint to range from 1 to 4.3 mm.<sup>2,4,20,28,29,36</sup> The 2.5-mm magnitude was chosen for this study as a midpoint in that range; this magnitude of facet retraction does not produce mechanical failure or visible rupture.<sup>28</sup> After retraction, each specimen was reoriented for the tensile configuration, and the same cyclic tensile loading protocol was repeated in order to assess changes in the mechanical response of the joint following retraction (Fig. 1). Prior to each loading scenario, images were acquired to ensure that the in situ joint position defined by the fiduciary pin locations remained consistent. Force and displacement data were acquired at 1 kHz during all loading configurations. Each

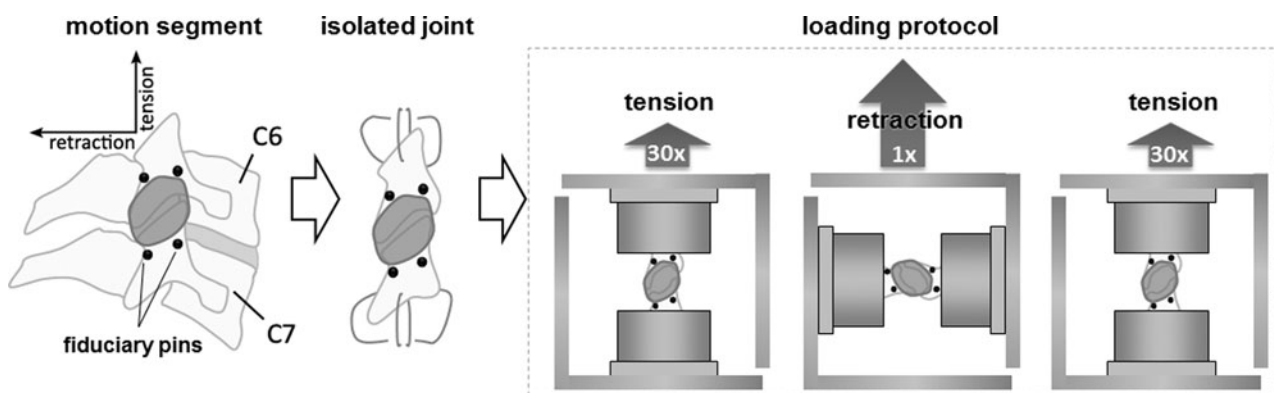


**FIGURE 1.** Isolated facet joints loaded in retraction and tension. Fiduciary pins were used to ensure that the joint's original configuration was maintained during testing. Cyclic tension in the axial direction was applied to pre-condition the joint. After a 90° rotation of the specimen, 2.5 mm of retraction was applied to the joint, corresponding to posterior shear loading of the vertebra. After retraction, the specimen was rotated back and cyclic tension was re-applied.

specimen was allowed to rest for 20 min between each loading protocol in order to allow re-hydration and viscoelastic recovery.<sup>11</sup> Pilot studies indicated that negligible changes in the force, stiffness, and laxity were detected between 20 min and 24 h after the application of retraction, confirming 20 min to be a sufficient recovery period.

#### *Analyses of Joint Mechanics and Fiber Kinematics During Retraction*

Joint mechanics, collagen fiber kinematics, and full-field capsule strains were acquired during facet joint retraction. The force–displacement data were analyzed to determine if ligament yield or failure occurred during retraction. Ligament yield was defined by any decrease in the tangent stiffness of at least 10% of the maximum recorded stiffness, and failure was defined by any decrease in force with increasing displacement.<sup>23</sup> Any occurrences of yield or failure during the joint retraction were documented, and the force at 2.5 mm was also recorded for each specimen.

Vector correlation of consecutive fiber alignment maps during retraction was used to assess anomalous fiber realignment as previously described.<sup>23</sup> In regions of the joint where articular bone could not be removed, insufficient light transmission prohibited polarized light analysis; such regions were defined by pixels where the harmonic polarized light intensity exhibited a signal-to-noise ratio (SNR) of less than 10. The vector correlation values obtained from all specimens in the unloaded state were used to determine the threshold for anomalous fiber realignment.<sup>23</sup> Anomalous realignment was defined at any pixel with an SNR greater than or equal to 10 and a decrease in vector correlation between maps of at least 0.35. The identification of anomalous realignment required the detection of a decrease in vector correlation in at least nine connected pixels simultaneously in order to eliminate potential random noise. For each specimen, the anatomical location and mechanical conditions corresponding to the detection of anomalous fiber realignment during retraction were noted.

Tissue deformation was defined during retraction by tracking the displacements of distinct fiber alignment patterns within the tissue as described previously.<sup>24</sup> Briefly, a grid of virtual markers with 4-pixel spacing was assigned to the first alignment map created from the QPLI images.<sup>24</sup> The fiber alignment within a  $9 \times 9$  pixel window surrounding each virtual marker was correlated with the fiber alignment in the subsequent frame. Marker displacements were calculated by maximizing the correlation of the local fiber alignment pattern between maps during the retraction.<sup>24</sup> A mesh of three-node elements was generated to estimate

strains through Delaunay triangulation using the virtual marker positions in the first alignment map. Using plane strain theory, Green's strain tensor was derived for each element in each alignment map. First principal strain ( $\epsilon_1$ ) and maximum shear strain ( $\gamma_{\max}$ ) were calculated to evaluate their utility in predicting the location of anomalous fiber realignment during retraction or altered fiber alignment remaining after retraction. First principal strain ( $\epsilon_1$ ) was determined from the maximum eigenvalue of an element's strain tensor, and  $\gamma_{\max}$  was defined as one-half of the difference between the two eigenvalues. At 2.5 mm of retraction,  $\epsilon_1$  and  $\gamma_{\max}$  were calculated for each node in the alignment map, and the average and maximum values for  $\epsilon_1$  and  $\gamma_{\max}$  were tabulated for each specimen.

#### *Analyses of Altered Joint Function & Microstructure Measured After Retraction*

Peak force, tangent stiffness, and laxity were determined from the final cycle for each of the tensile loading protocols before and after retraction to identify if altered ligament function was produced by joint retraction (Fig. 1). Data were only taken from the final (30th) cycle in order to eliminate any confounding effects due to the viscoelasticity of the tissue. To determine the laxity of each facet capsular ligament, a single reference load for measurements before and after retraction was defined by the force at 0.5 mm during the 1st cycle of loading prior to any retraction. Laxity was defined by any increase in displacement needed to produce that reference load,<sup>5,12</sup> and was measured at the 30th cycle of tensile loading. Tangent stiffness of the capsular ligament was calculated from the mid-point of the force–displacement curve at 0.5 mm. Differences between the peak force, stiffness, and laxity before and after retraction were compared at the 30th cycle using paired *t* tests.

In order to characterize microstructural evidence of ligament damage that may be induced by whiplash-like joint loading, unrecovered strain and altered fiber alignment were assessed between the alignment maps that were acquired before and after retraction. Virtual markers were tracked through a sequence of five alignment maps: two maps acquired before the retraction, two maps acquired after retraction, and a map acquired in the static unloaded configuration *before* retraction to ensure that any differences in the maps before and after retraction could be separated from the potential propagation of tracking error. If the position of a virtual marker differed by more than 0.5 pixels between the first and last maps in the series (both taken before retraction), the virtual marker position was deemed unstable and removed from the analysis. This tracking requirement ensured that only virtual



markers placed over capsule tissue with measureable birefringence were used for the strain and fiber alignment analyses. Using the same mesh generated for capsule strain measurements during joint retraction,  $\varepsilon_1$  and  $\gamma_{\max}$  were calculated at each virtual marker for the sequence of alignment maps. In order to make a direct comparison to the collagen fiber alignment surrounding a virtual marker, the local strains surrounding each marker were calculated by averaging the strain tensor values from all elements constructed using the node based on that marker. In addition, the vector correlation values between the positions of each virtual maker in each alignment map were recorded. A change in the vector correlation of a virtual marker between maps was used to determine the extent to which the fiber alignment surrounding that marker had changed after retraction.<sup>24</sup>

Full-field maps of  $\varepsilon_1$ ,  $\gamma_{\max}$ , and the change in vector correlation after retraction were generated for each specimen. In those maps, a node was classified as sustaining either unrecovered strain or altered fiber alignment after retraction if the value at that node exceeded the measurement's entire distribution of error values obtained from all nodes in all specimens. Errors for  $\varepsilon_1$  and  $\gamma_{\max}$  were determined from the strain field in the last of the five alignment maps used for vector correlation tracking, corresponding to the static unloaded configuration before retraction. The maximum  $\varepsilon_1$  or  $\gamma_{\max}$  recorded at any node in any specimen did not exceed 0.09 at this last alignment map so any node with  $\varepsilon_1$  or  $\gamma_{\max}$  greater than 0.09 after retraction was identified as having unrecovered  $\varepsilon_1$  or unrecovered  $\gamma_{\max}$ . Similarly, any node with a change in vector correlation that decreased below  $-0.10$  after retraction was defined as having sustained altered fiber alignment based on correlation error measurements from the maps acquired before retraction. These thresholds were also verified as appropriate through parametric analysis of the threshold value and the percentage of nodes that were detected as exceeding the threshold. For each specimen, the percentage of nodes with unrecovered  $\varepsilon_1$ , unrecovered  $\gamma_{\max}$ , and altered fiber alignment were determined.

To determine whether altered fiber alignment was co-localized with either unrecovered  $\varepsilon_1$  or  $\gamma_{\max}$ , two-by-two contingency tables were constructed, and Pearson's  $\chi^2$  tests were used to determine whether altered fiber alignment was associated with either unrecovered  $\varepsilon_1$  or  $\gamma_{\max}$ . Also, to determine whether altered fiber alignment was associated with higher strains during retraction, the strains that were sustained at 2.5 mm of retraction were compared between the nodes classified with altered alignment and the nodes without any detectable changes in alignment using a two-way ANOVA of alignment classification,

specimens, and their interaction. For both  $\varepsilon_1$  and  $\gamma_{\max}$  measurements, the same ANOVA structure was used to compare the strains at 2.5 mm of retraction among nodes with unrecovered and recovered strain after retraction. Significance was defined by  $\alpha = 0.05$  for all tests.

## RESULTS

During retraction, neither yield nor failure was detected, and the peak force at 2.5 mm retraction reached an average of  $16.08 \pm 9.83$  N (Table 1). Anomalous fiber realignment was not detected in any alignment map acquired during retraction for any specimen. An average of  $312 \pm 158$  virtual markers were assigned to each capsular ligament specimen and tracked during the retraction motion. At 2.5 mm of retraction, the average  $\varepsilon_1$  was  $0.42 \pm 0.23$  and the average  $\gamma_{\max}$  was  $0.28 \pm 0.10$  (Table 1). The full field  $\varepsilon_1$  and  $\gamma_{\max}$  measurements exhibited substantial spatial variability, with each specimen's maximum  $\varepsilon_1$  and  $\gamma_{\max}$  averaging  $2.18 \pm 0.79$  and  $1.14 \pm 0.36$ , respectively (Table 1; Fig. 2).

Joint retraction produced significant changes in the mechanical response of the capsular ligament to cyclic tensile loading. The peak force during the final cycle of tension decreased significantly ( $p = 0.0246$ ) from  $4.75 \pm 3.74$  N before retraction to  $3.99 \pm 3.15$  N after retraction (Table 2). The tangent stiffness in the final cycle also decreased significantly ( $p = 0.0186$ ) from  $2.85 \pm 2.68$  N/mm before retraction to  $2.08 \pm 2.28$  N/mm after retraction (Table 2). In addition, ligament laxity significantly increased ( $p = 0.0065$ ) from  $0.10 \pm 0.03$  mm in the final cycle before retraction to  $0.15 \pm 0.07$  mm in the corresponding cycle after retraction (Table 2).

After joint retraction, an average  $\varepsilon_1$  of  $0.06 \pm 0.04$  and an average  $\gamma_{\max}$  of  $0.05 \pm 0.02$  were detected in the

**TABLE 1. Force and strains ( $\varepsilon_1$  and  $\gamma_{\max}$ ) at 2.5 mm retraction.**

Specimen	Force (N)	Average		Maximum	
		$\varepsilon_1$	$\gamma_{\max}$	$\varepsilon_1$	$\gamma_{\max}$
17	10.99	0.41	0.26	3.24	1.58
18	31.84	0.30	0.18	1.70	0.95
19	23.12	0.84	0.44	1.76	0.86
20	5.38	0.41	0.28	1.55	0.86
21	4.74	0.72	0.42	2.66	1.36
22	13.93	0.19	0.18	1.28	0.71
23	12.82	0.26	0.21	3.33	1.69
24	25.80	0.26	0.25	1.88	1.11
Mean	16.08	0.42	0.28	2.18	1.14
SD	9.83	0.23	0.10	0.79	0.36

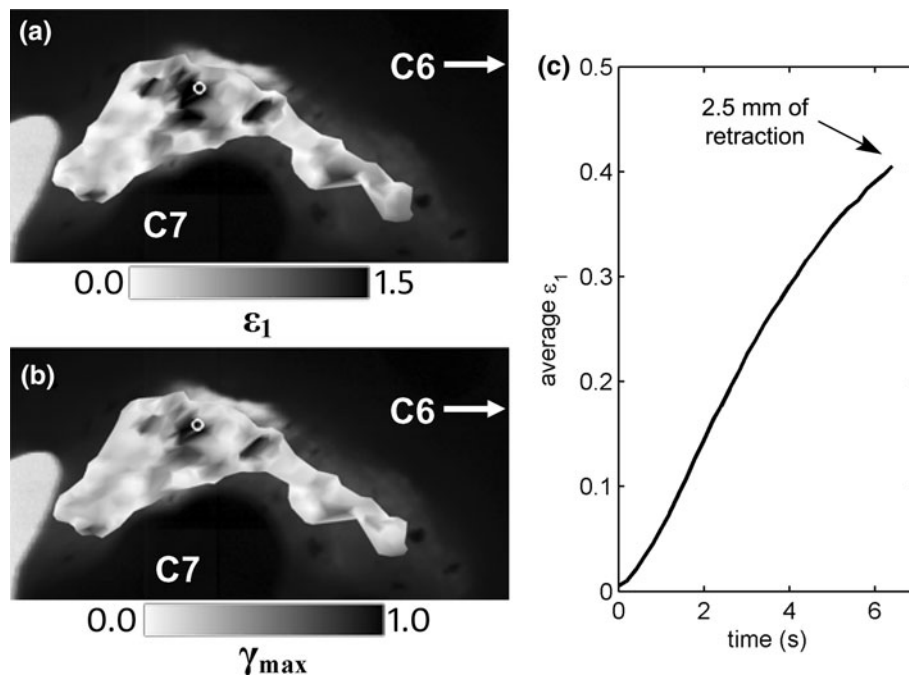


**FIGURE 2.** Full-field strain maps of (a)  $\varepsilon_1$  and (b)  $\gamma_{\max}$  at 2.5 mm retraction and (c) the time-history of the average  $\varepsilon_1$  applied during retraction (Specimen #17). The location of the maximum of each metric in (a) and (b) is circled; the retraction direction is shown (arrow).

**TABLE 2.** Mechanical outcomes for final cycle of tensile loading before and after retraction.

Specimen	Force (N)		Stiffness (N/mm)		Laxity (mm)	
	Before	After	Before	After	Before	After
17	2.15	1.52	1.69	1.00	0.11	0.26
18	4.72	4.05	2.93	2.26	0.09	0.15
19	7.57	6.34	3.73	2.39	0.15	0.21
20	0.25	0.35	0.09	0.13	0.05	0.03
21	2.51	2.21	1.18	0.84	0.08	0.14
22	9.13	6.84	4.06	1.96	0.10	0.21
23	1.56	1.42	0.70	0.68	0.08	0.09
24	10.08	9.17	8.47	7.34	0.10	0.14
Mean	4.75	3.99*	2.85	2.08*	0.10	0.15*
SD	3.74	3.15	2.68	2.28	0.03	0.07

\*Significant difference compared to mean value before retraction.

capsular ligament (Table 3). Strain varied substantially throughout the tissue for both measurements (Fig. 3); the maximum  $\varepsilon_1$  after retraction was  $0.93 \pm 0.82$  and the corresponding maximum  $\gamma_{\max}$  was  $0.47 \pm 0.39$  (Table 3). There were no trends in the location of the maximum  $\varepsilon_1$  and  $\gamma_{\max}$  after retraction. Every specimen contained nodes with unrecovered strain after retraction (Table 3). In fact,  $21.05 \pm 17.09\%$  of the nodes sustained unrecovered  $\varepsilon_1$  and  $14.07 \pm 11.49\%$  of the nodes were detected to have unrecovered  $\gamma_{\max}$  (Table 3). The average change in vector correlation between fiber alignment before and after retraction

**TABLE 3.** Unrecovered strain ( $\varepsilon_1$  and  $\gamma_{\max}$ ) after retraction.

Specimen	Average		Maximum		% of nodes unrecovered	
	$\varepsilon_1$	$\gamma_{\max}$	$\varepsilon_1$	$\gamma_{\max}$	$\varepsilon_1$	$\gamma_{\max}$
17	0.06	0.05	1.17	0.58	22.61	11.59
18	0.04	0.04	0.31	0.18	11.98	3.65
19	0.12	0.08	0.37	0.20	56.60	35.85
20	0.02	0.04	0.19	0.15	5.73	5.10
21	0.09	0.07	1.27	0.59	31.70	21.13
22	0.02	0.03	0.43	0.24	4.89	2.55
23	0.08	0.06	2.67	1.31	11.96	10.84
24	0.08	0.07	1.07	0.54	22.92	21.88
Mean	0.06	0.05	0.93	0.47	21.05	14.07
SD	0.04	0.02	0.82	0.39	17.09	11.49

was  $-0.09 \pm 0.04$ , and the average maximum decrease in the vector correlation of a node was  $-0.33 \pm 0.04$  (Table 4). As with unrecovered strain, the change in vector correlation after retraction varied spatially for each specimen (Fig. 3). After joint retraction,  $32.67 \pm 22.95\%$  of the nodes exceeded the threshold for altered fiber alignment (Table 4).

The majority of nodes with unrecovered  $\varepsilon_1$  or  $\gamma_{\max}$  also sustained altered fiber alignment (Table 5). In fact, the location of altered fiber realignment was significantly associated ( $p < 0.0001$ ) with the locations of both unrecovered  $\varepsilon_1$  and  $\gamma_{\max}$ , based on contingency table analysis (Table 5). Nodes with unrecovered  $\varepsilon_1$

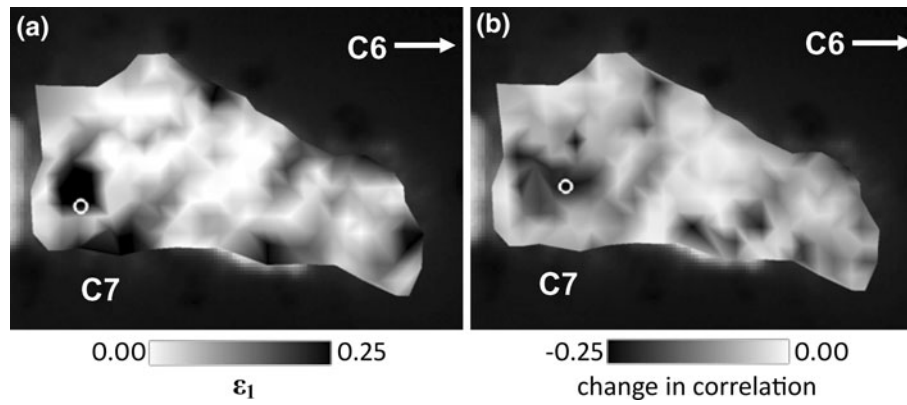


**FIGURE 3.** Maps of (a) full field  $\varepsilon_1$  and (b) the change in vector correlation for Specimen #21 after retraction. The maximum  $\varepsilon_1$  for this specimen is 0.59 and is circled in (a). The location of the greatest decrease in correlation indicates the greatest change in fiber alignment and is circled in (b). The arrows indicate the C6 facet retraction direction.

**TABLE 4.** Change in vector correlation of fiber alignment after retraction.

Specimen	Average change in correlation	Maximum decrease in correlation	% of nodes with altered alignment
17	-0.09	-0.35	32.17
18	-0.08	-0.36	24.74
19	-0.17	-0.36	86.79
20	-0.09	-0.27	28.03
21	-0.09	-0.31	30.94
22	-0.05	-0.34	11.91
23	-0.06	-0.34	17.57
24	-0.07	-0.27	29.17
Mean	-0.09	-0.33	32.67
SD	0.04	0.04	22.95

**TABLE 5.** Co-localization of unrecovered strain and altered fiber alignment after retraction.

Altered fiber alignment	Unrecovered $\varepsilon_1$			Unrecovered $\gamma_{\max}$		
	Yes	No	Total	Yes	No	Total
Yes	228	384	612	192	420	612
No	172	1713	1885	78	1807	1885
Total	400	2097	2497	270	2227	2497

after retraction experienced a significantly higher ( $p = 0.0399$ )  $\varepsilon_1$  at peak retraction ( $0.49 \pm 0.47$ ) than the nodes where strain was recovered ( $0.32 \pm 0.39$ ) upon unloading (Fig. 4). In addition, nodes with unrecovered  $\gamma_{\max}$  after retraction sustained significantly higher ( $p = 0.0110$ )  $\gamma_{\max}$  at peak retraction ( $0.32 \pm 0.21$ ) than compared to nodes without unrecovered  $\gamma_{\max}$  ( $0.23 \pm 0.19$ ). However, no significant differences in the strains at peak retraction were identified between nodes with altered and unaltered

fiber alignment after retraction ( $p = 0.0860$  for  $\varepsilon_1$ ;  $p = 0.0983$  for  $\gamma_{\max}$ ) (Fig. 4).

## DISCUSSION

This study used quantitative polarized light imaging to demonstrate that whiplash-like vertebral retraction *can* produce altered collagen fiber alignment in the facet capsular ligament (Table 4; Fig. 3), which is associated with significant laxity and reduced ligament stiffness (Table 2). The proportion of the capsule that sustained altered fiber alignment after retraction ranged from 11.91 to 86.79%, representing a substantial rearrangement of the collagen organization in the facet capsule for some specimens (Table 4). Tissue regions with altered fiber alignment after retraction were also significantly co-localized ( $p < 0.0001$ ) with the regions in which unrecovered strain after retraction was also detected (Table 5). This spatial association suggests that changes in the microstructural organization after retraction may contribute to the altered mechanical function. Previous studies have identified anomalous collagen fiber realignment during loading prior to capsule failure or visible rupture,<sup>23</sup> but neither capsule failure nor anomalous fiber realignment was detected to occur *during* whiplash-like retraction in the current study. The absence of any mechanical or image-based evidence of collagen fiber damage during retraction in our study may indicate that the permanent deformation of ground substance materials comprising the ligament led to the altered collagen fiber organization detected after retraction (Fig. 3). It still remains unknown whether the changes in fiber organization are the result of tissue damage sufficient to induce an inflammatory response or nociceptor firing in the ligament. Although the underlying mechanism that

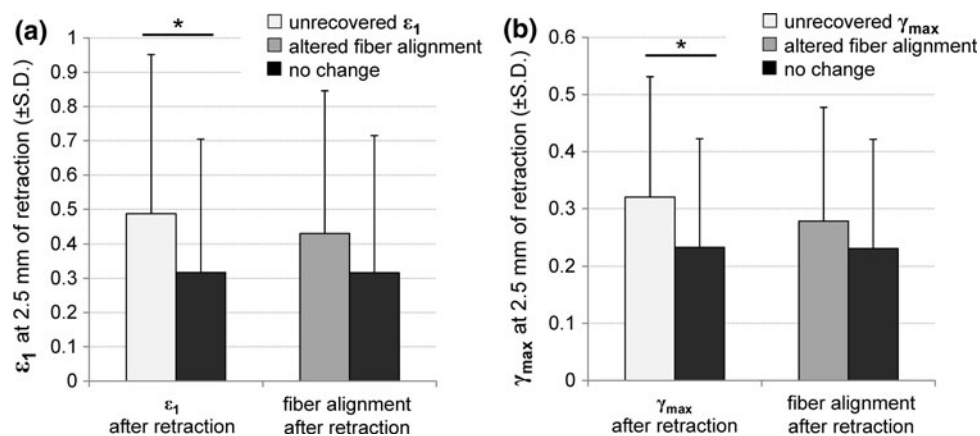


**FIGURE 4. Unrecovered strain after retraction was associated with higher strains during retraction, but altered fiber alignment was not associated with significantly higher strains. (a) Nodes with unrecovered  $\epsilon_1$  after retraction sustained significantly higher  $\epsilon_1$  values at 2.5 mm of retraction ( $*p = 0.0399$ ) compared to nodes in which strain was recovered. (b) Unrecovered  $\gamma_{max}$  after retraction also corresponded to significantly higher ( $*p = 0.0110$ )  $\gamma_{max}$  during retraction compared to nodes without changes in strain.**

produced altered collagen fiber alignment and unrecovered strain in the current study remains unknown (Fig. 3; Tables 3, 4), the optical imaging findings documented here do provide the first evidence of a change in the facet capsule microstructure following a whiplash-like joint retraction.

The production of facet capsular ligament laxity following a whiplash-like retraction in this study (Table 2) is consistent with previous findings of facet joint laxity following inertial loading of isolated cervical spines.<sup>12</sup> The production of joint laxity may indicate the potential for radiographic abnormalities in whiplash patients that have been previously documented, including modifications to the facet joint spacing or cervical spine angulation.<sup>10,35</sup> However, any irregularities in the cervical spine curvature of whiplash patients in clinical studies may be the result of compensatory mechanisms related to muscle spasms or neck pain rather than direct indications of tissue damage.<sup>10,25</sup> Furthermore, variations in the cervical spine curvature in whiplash patients often cannot be distinguished from the normal variations observed for asymptomatic individuals.<sup>19</sup> Collectively, the majority of radiographic or MRI studies involving whiplash patients identify little, if any, direct evidence of structural damage to the soft tissues in the neck.<sup>21,25</sup> In contrast, polarized light imaging demonstrated changes in the collagen fiber alignment of every capsular ligament specimen in this study following whiplash-like loading by correlating fiber alignment patterns within  $0.25 \text{ mm}^2$  tissue regions (Table 4). These findings would suggest that radiographic or MRI diagnostic approaches may lack the resolution to detect the microstructural changes that can occur in the facet capsule without overt capsule rupture after a whiplash exposure.

Although capsule regions with unrecovered strain after retraction sustained greater strain magnitudes at

peak facet retraction in this study ( $p = 0.0399$ ), significantly higher strains *during* retraction were not sustained by the regions with altered fiber alignment (Fig. 4). This lack of an association between the changes in the fiber organization *after* retraction and the capsule strains *during* retraction parallels the difference in locations of anomalous fiber realignment and maximum  $\epsilon_1$  identified for the human cervical capsule loaded in tension in previous work.<sup>23</sup> Collectively, both of these QPLI studies of the facet capsular ligament suggest that the location of maximum principal strain ( $\epsilon_1$ ) at the macro-scale level may differ from the location of maximum principal strain at the micro-scale level due to regional differences in fiber orientation and organization. The disconnect between macro-scale strain and the location of ligament damage suggests that traditional finite element models of the facet capsule using linear elastic<sup>8</sup> or non-linear spring elements<sup>32</sup> will not have the capability to accurately localize ligament injury. However, fiber-based models can simulate the microstructural kinematics of the facet capsule,<sup>7</sup> but the number of fibers required to model the complex fiber network organization<sup>23</sup> of the capsular ligament may be too computational demanding. By developing image-based multi-scale fiber network models, the tissue-level and fiber-level stress-strain responses in engineered constructs have been predicted under complex loading conditions.<sup>27</sup> The implementation of a similar QPLI-based model for the facet capsular ligament may help to further illuminate the reasons behind these differences in the locations of strain maxima and microstructural damage during loading.

Both the magnitude (2.5 mm) and the quasi-static rate (0.4 mm/s) of facet joint retraction used in this study were chosen to approximate previous whiplash simulations using whole cadavers or isolated spinal



motion segments.<sup>28,29</sup> However, the complete range of neck motions during a rear-end impact occur over 200 ms and involve more complex bony kinematics that can include compression and joint sliding in addition to retraction.<sup>4,20,29</sup> Additional studies imposing the more complex joint loading motions that include joint sliding, compression, and sagittal rotations may help to further evaluate the potential for microstructural damage during the whiplash kinematic. Although capsule stress may be greater for higher joint loading rates than used here, the displacements required for capsule failure have been shown to not differ between dynamic and quasi-static loading.<sup>34</sup> If capsule failure properties are indeed more dependent on the displacements or strains than on stress, the quasi-static loading imposed in the current study is likely a sufficient model of the conditions that could produce potential tissue damage during whiplash. Future work comparing the fiber alignment of the facet capsule before and after a high-speed retraction motion can help to confirm this assumption. Finally, this study evaluated the mechanical and microstructural properties of only a single spinal level (C6/C7). Although the failure properties of the lower cervical facet joints do not differ,<sup>28,34</sup> additional experiments are needed to investigate whether the same holds for microstructural responses and for injury in the upper cervical spine.

The maximum  $\varepsilon_1$  measured ( $2.18 \pm 0.79$ ) in isolated specimens in the current study (Table 1) was substantially greater than the maximum  $\varepsilon_1$  sustained at peak retraction ( $0.178 \pm 0.058$ ) in previous studies of capsule deformation during facet joint retraction.<sup>28</sup> The finer spatial resolution ( $312 \pm 158$  markers) afforded by the vector correlation tracking used in this study is an order of magnitude greater than the marker resolution of previous facet capsule measurements and may explain the range of strain values estimated here being greater than previously reported for facet capsule deformation under retraction or tension.<sup>28,34</sup> The discrepancy between maximum strain values suggests that macro-scale strain measurements may not fully capture the deformation gradients associated with microstructural ligament damage under these loading conditions. The average  $\varepsilon_1$  in each specimen at 2.5 mm of retraction ( $0.42 \pm 0.23$ ) is below the magnitude required to produce anomalous fiber realignment ( $0.503 \pm 0.238$ ) or failure ( $1.12 \pm 0.43$ ) in previous tensile failure studies,<sup>23,24</sup> which explains the absence of any detection of anomalous realignment during retraction in this study. Although the average strain produced in this study is lower than that required to produce anomalous fiber realignment of capsule ruptures during loading, it is consistent with the magnitude of strain reported for the C6/C7 facet joint (0.399) during a

simulation of whiplash loading to the cervical spine via inertial loading.<sup>20</sup> Although the average strain values derived from fiber alignment tracking in this study are consistent with previous work, these findings suggest many challenges in defining and localizing sub-catastrophic ligament injuries based on macro-scale strain field data; this work further highlights the need for image-based methods to directly detect painful injuries rather than using traditional mechanical engineering approaches.

Aside from the co-localization of unrecovered  $\varepsilon_1$  and  $\gamma_{\max}$  with altered fiber alignment, no trends in the anatomical location of unrecovered strain were identified (Fig. 3). Yet, for a small percentage of each capsule, large plastic deformations may have been produced by whiplash-like retraction given the maximum unrecovered  $\varepsilon_1$  and  $\gamma_{\max}$  detected after retraction (Table 3). The magnitude of the maximum unrecovered  $\varepsilon_1$  in over half of the specimens (Table 3) exceeded the strain threshold reported to activate nociceptor firing defined in a goat model of facet capsule stretch.<sup>18</sup> In addition, previous work with a rat model has demonstrated that facet joint displacements that produce persistent pain symptoms also induce laxity in the capsular ligament and collagen fiber disorganization.<sup>15,16,22</sup> When placed in the context of these other *in vivo* studies, the detection of altered fiber alignment and unrecovered strain observed after facet retraction in the current study would suggest that whiplash-like loading may be sufficient to generate facet-mediated pain. However, additional *in vivo* and/or clinical studies are required to test the relationship between altered collagen alignment and facet-mediated pain. Although QPLI requires the transmission of polarized light through ligament tissue, non-linear optical microscopy and optical coherence tomography may enable non-invasive measurements of the collagen microstructure *in vivo*. Furthermore, the use of minimally invasive fiber optic probes for non-linear optical imaging may enable quantitative measurements of collagen organization in future clinical imaging approaches.<sup>17</sup>

By identifying altered fiber alignment *after* joint retraction (Table 4), in addition to assessing potential anomalous realignment *during* retraction, this polarized light imaging study demonstrates that microstructural changes to the facet capsule can be produced by whiplash-like loading. Interestingly, anomalous fiber realignment *during* loading was not detected in any specimen and may not be a requisite for the altered fiber alignment and unrecovered mechanical changes that were detected *after* retraction in this study. Yet, the co-localization of unrecovered strain and altered fiber alignment in the current study (Fig. 3; Table 5) suggests that the development of laxity in this and

other simulations of whiplash may be the result of microstructural damage. The assessment of altered fiber alignment is derived from the ability to calculate the correlation of the same tissue region before and after loading through vector correlation tracking. Accordingly, the vector correlation analyses employed here cannot be implemented in a clinical setting to diagnose whiplash-associated disorders. Additionally, substantial specimen-to-specimen variability was observed in the force, strain, and fiber-based measurements obtained in this study (Tables 1, 2, 3, 4; Fig. 4), and the ability to make pair-wise comparisons before and after retraction provided the statistical power to identify evidence of microstructural injury. This variability among specimens is consistent with other reports for this ligament<sup>4,12,23,24,28,34</sup> and suggests that the development of whiplash-induced laxity or altered fiber alignment may not be detectable in a clinical setting using current approaches. Nonetheless, a mechanistic understanding of how and when microstructural injuries occur during whiplash-like motion can be established through these microstructural imaging techniques, which should aid in developing and validating new diagnostic tools capable of detecting these subtle, mechanically induced structural changes.

#### ACKNOWLEDGMENTS

This material is based on work supported by and the National Science Foundation under Grant no. 0547451, and was also funded by support from the Catharine D. Sharpe Foundation, the Association for the Advancement of Automotive Medicine, and the Defense University Research Instrumentation Program of the U.S. Army Research Office.

#### REFERENCES

- <sup>1</sup>Barnsley, L., S. Lord, and N. Bogduk. Whiplash injury. *Pain* 58:283–307, 1994.
- <sup>2</sup>Bogduk, N., and N. Yoganandan. Biomechanics of the cervical spine. Part 3: minor injuries. *Clin. Biomech.* 16:267–275, 2001.
- <sup>3</sup>Croft, P. R., M. Lewis, A. C. Papageorgiou, E. Thomas, M. I. Jayson, G. J. Macfarlane, and A. J. Silman. Risk factors for neck pain: a longitudinal study in the general population. *Pain* 93:317–325, 2001.
- <sup>4</sup>Deng, B., P. C. Begeman, K. H. Yang, S. Tashman, and A. I. King. Kinematics of human cadaver cervical spine during low speed rear-end impacts. *Stapp Car Crash J.* 44:171–188, 2000.
- <sup>5</sup>Eagar, P., M. L. Hull, and S. M. Howell. A method for quantifying the anterior load-displacement behavior of the human knee in both the low and high stiffness regions. *J. Biomech.* 34:1655–1660, 2001.
- <sup>6</sup>Gargan, M. F., and G. C. Bannister. The rate of recovery following whiplash injury. *Eur. Spine J.* 3:162–164, 1994.
- <sup>7</sup>Goel, V. K., T. M. Yamanishi, and H. Chang. Development of a computer model to predict strains in the individual fibers of a ligament across the ligamentous occipito-atlanto-axial (C0-C1-C2) complex. *Ann. Biomed. Eng.* 20:667–686, 1992.
- <sup>8</sup>Greaves, C. Y., M. S. Gadala, and T. R. Oxland. A three-dimensional finite element model of the cervical spine with spinal cord: an investigation of three injury mechanisms. *Ann. Biomed. Eng.* 36:396–405, 2008.
- <sup>9</sup>Guzman, J., S. Haldeman, L. J. Carroll, E. J. Carragee, E. L. Hurwitz, P. Peloso, M. Nordin, J. D. Cassidy, L. W. Holm, P. Cote, G. van der Velde, and S. Hogg-Johnson. Clinical practice implications of the Bone and Joint Decade 2000–2010 Task Force on Neck Pain and Its Associated Disorders: from concepts and findings to recommendations. *Spine* 33:S199–S213, 2008.
- <sup>10</sup>Helliwell, P. S., P. F. Evans, and V. Wright. The straight cervical spine: does it indicate muscle spasm? *J. Bone Joint Surg. Br.* 76:103–106, 1994.
- <sup>11</sup>Iatridis, J. C., J. J. MacLean, and D. A. Ryan. Mechanical damage to the intervertebral disc annulus fibrosus subjected to tensile loading. *J. Biomech.* 38:557–565, 2005.
- <sup>12</sup>Ivancic, P. C., S. Ito, Y. Tominaga, W. Rubin, M. P. Coe, A. B. Ndu, E. J. Carlson, and M. M. Panjabi. Whiplash causes increased laxity of cervical capsular ligament. *Clin. Biomech.* 23:159–165, 2008.
- <sup>13</sup>Kaneoka, K., K. Ono, S. Inami, and K. Hayashi. Motion analysis of cervical vertebrae during whiplash loading. *Spine* 24:763–769, 1999.
- <sup>14</sup>Lake, S. P., K. S. Miller, D. M. Elliott, and L. J. Soslow-sky. Effect of fiber distribution and realignment on the nonlinear and inhomogeneous mechanical properties of human supraspinatus tendon under longitudinal tensile loading. *J. Orthop. Res.* 27:1596–1602, 2009.
- <sup>15</sup>Lee, K. E., M. B. Davis, and B. A. Winkelstein. Capsular ligament involvement in the development of mechanical hyperalgesia after facet joint loading: behavioral and inflammatory outcomes in a rodent model of pain. *J. Neurotrauma* 25:1383–1393, 2008.
- <sup>16</sup>Lee, K. E., and B. A. Winkelstein. Joint distraction magnitude is associated with different behavioral outcomes and substance P levels for cervical facet joint loading in the rat. *J. Pain* 10:436–445, 2009.
- <sup>17</sup>Levene, M. J., D. A. Dombeck, K. A. Kasischke, R. P. Molloy, and W. W. Webb. In vivo multiphoton microscopy of deep brain tissue. *J. Neurophysiol.* 91:1908–1912, 2004.
- <sup>18</sup>Lu, Y., C. Chen, S. Kallakuri, A. Patwardhan, and J. M. Cavanaugh. Neural response of cervical facet joint capsule to stretch: a study of whiplash pain mechanism. *Stapp Car Crash J.* 49:49–65, 2005.
- <sup>19</sup>Matsumoto, M., Y. Fujimura, N. Suzuki, Y. Toyama, and H. Shiga. Cervical curvature in acute whiplash injuries: prospective comparative study with asymptomatic subjects. *Injury* 29:775–778, 1998.
- <sup>20</sup>Pearson, A. M., P. C. Ivancic, S. Ito, and M. M. Panjabi. Facet joint kinematics and injury mechanisms during simulated whiplash. *Spine* 29:390–397, 2004.
- <sup>21</sup>Pettersson, K., C. Hildingsson, G. Toolanen, M. Fagerlund, and J. Bjornebrink. Disc pathology after whiplash injury. A prospective magnetic resonance imaging and clinical investigation. *Spine* 22:283–287, 1997.

- <sup>22</sup>Quinn, K. P., K. E. Lee, C. C. Ahaghotu, and B. A. Winkelstein. Structural changes in the cervical facet capsular ligament: potential contributions to pain following subfailure loading. *Stapp Car Crash J.* 51:169–187, 2007.
- <sup>23</sup>Quinn, K. P., and B. A. Winkelstein. Vector correlation technique for pixel-wise detection of collagen fiber realignment during injurious tensile loading. *J. Biomed. Opt.* 14:054010, 2009.
- <sup>24</sup>Quinn, K. P., and B. A. Winkelstein. Full-field strain measurements of collagenous tissue by tracking fiber alignment through vector correlation. *J. Biomech.* 43:2637–2640, 2010.
- <sup>25</sup>Ronnen, H. R., P. J. de Korte, P. R. Brink, H. J. van der Bijl, A. J. Tonino, and C. L. Franke. Acute whiplash injury: is there a role for MR imaging? A prospective study of 100 patients. *Radiology* 201:93–96, 1996.
- <sup>26</sup>Rothman, S. M., and B. A. Winkelstein. Cytokine antagonism reduces pain and modulates spinal astrocytic reactivity after cervical nerve root compression. *Ann. Biomed. Eng.* 38:2563–2576, 2010.
- <sup>27</sup>Sander, E. A., T. Stylianopoulos, R. T. Tranquillo, and V. H. Barocas. Image-based multiscale modeling predicts tissue-level and network-level fiber reorganization in stretched cell-compacted collagen gels. *Proc. Natl. Acad. Sci. USA* 106:17675–17680, 2009.
- <sup>28</sup>Siegmund, G. P., B. S. Myers, M. B. Davis, H. F. Bohnet, and B. A. Winkelstein. Mechanical evidence of cervical facet capsule injury during whiplash: a cadaveric study using combined shear, compression, and extension loading. *Spine* 26:2095–2101, 2001.
- <sup>29</sup>Sundararajan, S., P. Prasad, C. K. Demetropoulos, S. Tashman, P. C. Begeman, K. H. Yang, and A. I. King. Effect of head-neck position on cervical facet stretch of post mortem human subjects during low speed rear end impacts. *Stapp Car Crash J.* 48:331–372, 2004.
- <sup>30</sup>Teo, E. C., and H. W. Ng. Evaluation of the role of ligaments, facets and disc nucleus in lower cervical spine under compression and sagittal moments using finite element method. *Med. Eng. Phys.* 23:155–164, 2001.
- <sup>31</sup>Tower, T. T., M. R. Neidert, and R. T. Tranquillo. Fiber alignment imaging during mechanical testing of soft tissues. *Ann. Biomed. Eng.* 30:1221–1233, 2002.
- <sup>32</sup>Wheeldon, J. A., B. D. Stemper, N. Yoganandan, and F. A. Pintar. Validation of a finite element model of the young normal lower cervical spine. *Ann. Biomed. Eng.* 36:1458–1469, 2008.
- <sup>33</sup>Whittaker, P., and P. B. Canham. Demonstration of quantitative fabric analysis of tendon collagen using two-dimensional polarized light microscopy. *Matrix* 11:56–62, 1991.
- <sup>34</sup>Winkelstein, B. A., R. W. Nightingale, W. J. Richardson, and B. S. Myers. The cervical facet capsule and its role in whiplash injury: a biomechanical investigation. *Spine* 25:1238–1246, 2000.
- <sup>35</sup>Yoganandan, N., J. F. Cusick, F. A. Pintar, and R. D. Rao. Whiplash injury determination with conventional spine imaging and cryomicrotomy. *Spine* 26:2443–2448, 2001.
- <sup>36</sup>Yoganandan, N., F. A. Pintar, and M. Klienberger. Cervical spine vertebral and facet joint kinematics under whiplash. *J. Biomech. Eng.* 120:305–307, 1998.
- <sup>37</sup>Zdeblick, T. A., J. J. Abitbol, D. N. Kunz, R. P. McCabe, and S. Garfin. Cervical stability after sequential capsule resection. *Spine* 18:2005–2008, 1993.